

The hyperbolic geometry of financial networks

Martin Keller-Ressel^{1,*} and Stephanie Nargang¹

¹TU Dresden, Institute for Mathematical Stochastics, Dresden, 01062, Germany

*martin.keller-ressel@tu-dresden.de

ABSTRACT

Based on data from the European banking stress tests of 2014, 2016 and the transparency exercise of 2018 we demonstrate for the first time that the latent geometry of financial networks can be well-represented by geometry of negative curvature, i.e., by hyperbolic geometry. This allows us to connect the network structure to the popularity-vs-similarity model of Papadopoulos et al., which is based on the Poincaré disc model of hyperbolic geometry. We show that the latent dimensions of ‘popularity’ and ‘similarity’ in this model are strongly associated to systemic importance and to geographic subdivisions of the banking system. In a longitudinal analysis over the time span from 2014 to 2018 we find that the systemic importance of individual banks has remained rather stable, while the peripheral community structure exhibits more (but still moderate) variability.

Introduction

Network models based on hyperbolic geometry have been successful in explaining the structural features of informational¹, social² and biological networks³. Such models provide a mathematical framework to resolve the conflicting paradigms of preferential attachment (attraction to *popular* nodes) and community effects (attraction to *similar* nodes) in networks.⁴⁻⁶ Just as the geometric structure of a social network determines the diffusion of news, rumors or infective diseases between individuals⁷, the geometric structure of a financial network influences the diffusion of financial stress between financial institutions, such as banks.⁸⁻¹⁰ Indeed, the lack of understanding for risks originating from the systemic interaction of financial institutions has been identified as a major contributing factor to the global financial crisis of 2008.¹¹ While many recent studies have analysed the mechanisms of financial contagion in theoretical or simulation-based settings, less attention has been paid to the structural and geometric characteristics of real financial networks. In particular, it has remained an open question, whether the paradigm of hyperbolic structure applies to financial and economic networks and what such a structure implies for financial contagion processes.

Here, we consider financial networks inferred from bank balance sheet data, as collected and made available by the European Banking Authority (EBA) within the European banking stress test and transparency exercises of 2014, 2016 and 2018.^{12,13} We show that these networks can be embedded into low-dimensional hyperbolic space with considerably smaller distortion than into Euclidean space, suggesting that the paradigm of latent hyperbolic geometry also applies to financial networks. Furthermore – following Papadopoulos et al.⁴ – we decompose the embedded hyperbolic coordinates into the dimensions of *popularity* and *similarity* and demonstrate that these dimensions align with *systemic importance* and membership in *regional banking clusters* respectively. Finally, the longitudinal structure of the data allows us to track changes in these dimensions over time, i.e., to track the stability of systemic importance and of the peripheral community structure over time.

Results

Inference of Financial Networks

Contagion in financial networks is a complex process, which can take place through several parallel (and potentially interacting) mechanisms and channels.¹⁴ These mechanisms include direct bank-to-bank liabilities¹⁵, bank runs¹⁶, and market-mediated contagion through asset sales^{14,17-19} (‘fire-sale contagion’); see also [11, p.21ff]. Here, we focus on the channel of fire-sale contagion, which has been singled out – both in simulation¹⁸ and in empirical studies¹⁷ – as a key mechanism of financial contagion. Moreover, the propensity of fire-sale contagion can be quantified from available balance sheet data, using liquidity-weighted portfolio overlap (LWPO)^{19,20} as an indicator (see Methods for details).

Our inference of financial networks follows a two-stage mechanism: First, we construct a weighted bipartite network in which banks $B = (b_1, \dots, b_n)$ are linked to a common pool of assets $A = (a_1, \dots, a_m)$, which consist of sovereign bonds classified by issuing country and by different levels of maturity. In the second step we perform a one-mode projection of this network on the node set B , using the LWPO of two banks $b_i, b_j \in B$ to determine the weight w_{ij} of the link between the corresponding nodes. For any of the years $y \in \{2014, 2016, 2018\}$, the result is an undirected, weighted network N_y of banks, in which two banks are connected if and only if they hold common assets. The link weight w_{ij} , normalized to $[0, 1]$, represents

the susceptibility of two banks b_i, b_j to financial contagion, quantified by their LWPO. The inferred networks are very dense, i.e., almost all pairs of banks hold *some* common assets. However, most of the connections have very small weights, and the networks are dominated by a ‘sparse backbone’ of a few strong connections, which represent the dominant channels of potential contagion of financial distress; see Figure 1.A.

Latent network geometry

Our first objective was to uncover the latent geometric network structure and to evaluate the suitability of a hyperbolic network model. (See Methods for background on hyperbolic geometry.) To this end, we calculated stress-minimizing embeddings of the financial networks N_{2014}, N_{2016} and N_{2018} into two-dimensional Euclidean space \mathbb{E}_2 and hyperbolic space \mathbb{H}_2 . These methods correspond to classic multidimensional scaling²¹ in the Euclidean case and to the `hydra+` embedding method^{22,23} in the hyperbolic case. The residual stress can be used as a goodness-of-fit measure between geometric model and true network topology. As shown in Figure 1.B the residual embedding stress from the hyperbolic model is substantially smaller – consistently over all three years of observation – than from the Euclidean model. This indicates that the latent geometry of the observed financial networks is much better represented by negatively curved (hyperbolic) rather than flat (Euclidean) geometry. It is also evidence of a high degree of hierarchical organization²⁴ in the financial networks considered. Furthermore, as a result of the embedding we obtain for each bank node b_i latent coordinates (r_i, θ_i) in the Poincaré disc model of hyperbolic space (see Methods), which allows us to connect the network embedding to the popularity-vs-similarity model of Papadopoulos et al.⁴ The hyperbolic embedding of the full banking network of 2018 is shown in Figure 2. The embedded network shows a clear core-periphery structure, in line with previous studies of financial networks.^{25,26} A deeper analysis of this structure is the subject of the following section.

Structural Analysis

The popularity-vs-similarity model of Papadopoulos et al.⁴ offers a direct interpretation of the latent hyperbolic network coordinates in the Poincaré disc in terms of their *popularity* dimension (the radial coordinate r) and the *similarity* dimension (the angular coordinate θ). In the context of financial networks, we hypothesized that the popularity dimension of a given bank aligns with its systemic importance, and that its similarity dimension is associated with sub-sectors of the banking system, e.g., along geographic and regional divisions. Due to the asymmetric distribution of banks within the Poincaré disc (Figure 2), we slightly adapt the model Papadopoulos et al.⁴ and calculate the geodesic polar coordinates (r'_i, θ'_i) with respect to the network center-of-weight, rather than the center of the Poincaré disc; see Methods for details.

Rank	2014	2016	2018
1	Nordea *	BNP Paribas *	Groupe BPCE *
2	Royal Bank of Scotland *	UniCredit *	Barclays *
3	Barclays *	ING Groep *	Royal Bank of Scotland
4	Intesa Sanpaolo	Deutsche Bank *	Groupe Crédit Agricole *
5	UniCredit *	Intesa Sanpaolo	BNP Paribas *

Table 1. For each year the five banks with the highest hyperbolic centrality (i.e. smallest r' coordinate) are listed. Asterisks denote banks that are considered globally systemic relevant institutions (G-SIBs)

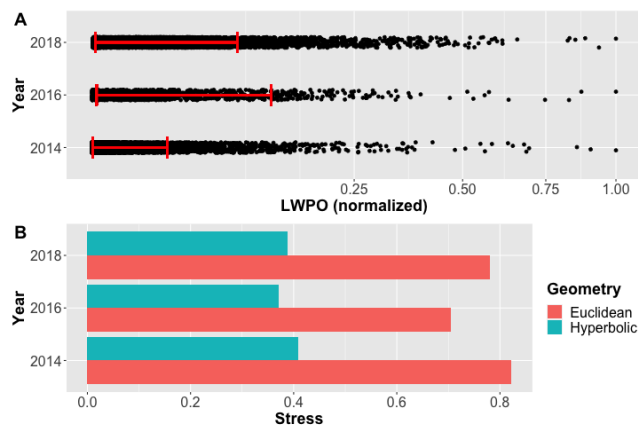


Figure 1. Panel A: Edge weight distribution in the EBA Networks of years 2014, 2016 and 2018. The inter-decile range of the (highly skewed) distributions is indicated in red. Panel B: Stress of network embedding into Euclidean vs. Hyperbolic geometry. Lower values of stress indicate better goodness-of-fit.

To test the first hypothesis – the association between radial coordinate r' and systemic importance – we labelled a bank as *systemically important* in a given year, whenever it was included in the contemporaneous list of global systemically important banks (G-SIBs) as published by the Financial Stability Board.^{27–29}; see also Table 3. Using a Wilcoxon–Mann–Whitney test, we find a significant association between radial rank and systemic importance in all years ($P_{2014} < .0001$, $P_{2016} < .0001$, $P_{2018} = .0038$). In Table 1 we report the five top-ranked banks (most central in terms of r') for each year.

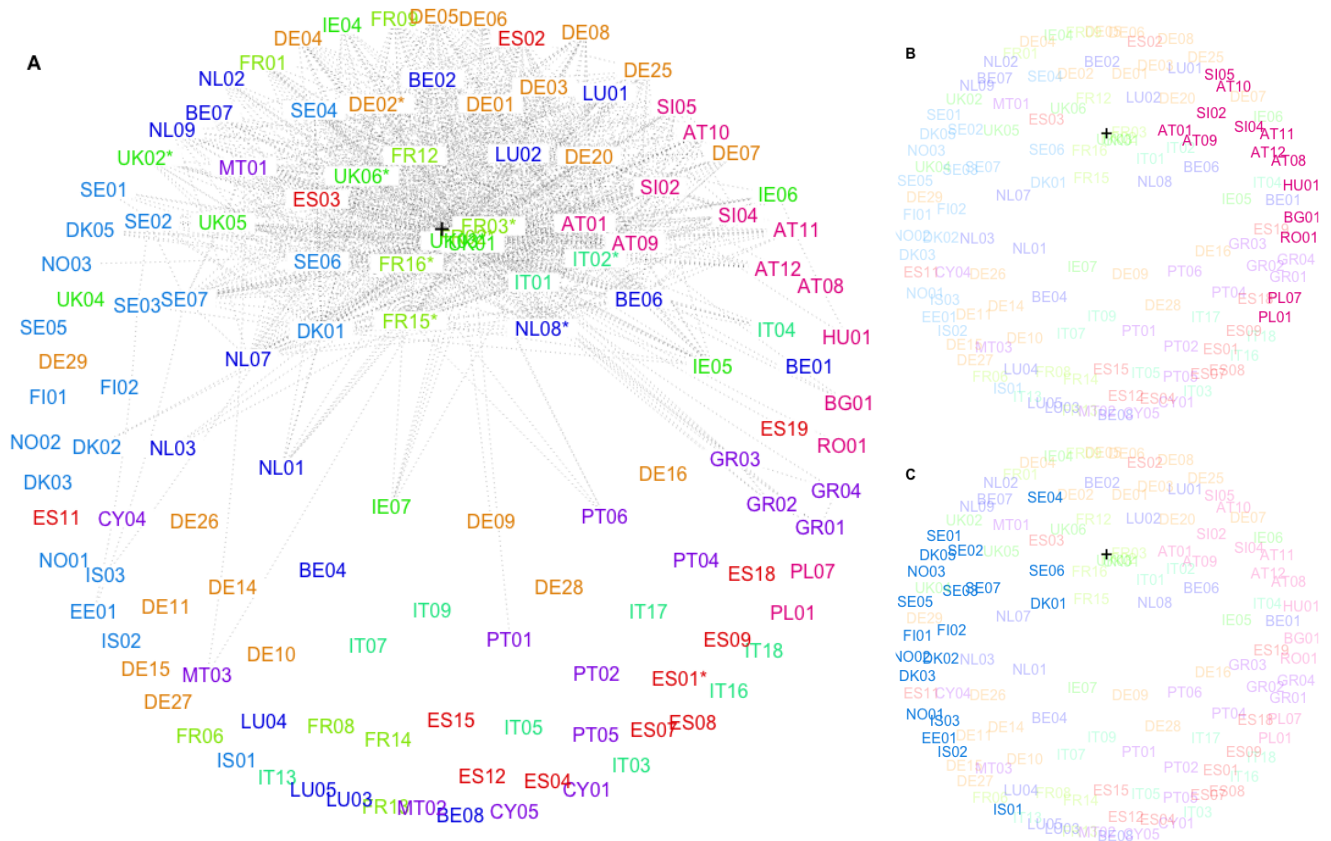


Figure 2. Hyperbolic Embedding of the EBA Financial Network of 2018. Nodes are labelled by country and bank ID and coloured according to region (see Table 3 for full names). Panel A shows the full network including the strongest links (top decile), i.e., the connections with the largest liquidity-weighted portfolio overlap. Banks labelled as systemically important by the Financial Stability Board (G-SIBs) are indicated by asterisks. The black cross marks the capital-weighted hyperbolic center of the banking network. In panels B and C the Central/Eastern and the Nordic regional groups are highlighted to illustrate regional clustering.

To test the second hypothesis – the association between similarity dimension θ' and regional banking sub-sectors – we assigned banks to the following nine regional groups:

Spain (ES), Germany (DE), France (FR), Italy (IT), UK and Ireland (UK/IE), Nordic Region (EE/NO/SE/DK/FI/IS), Benelux Region (BE/NE/LU), Southern/Mediterranean (GR/CY/MT/PT), Central and Eastern Europe (AT/BG/HU/LV/RO/SI).

These regions are reasonably balanced in terms of the number of banks included in the EBA panel. Using ANOVA for circular data [30, Sec. 7.4] we find a highly significant association between the angular coordinate θ' and the regional group in all three years considered ($P < .0001$ in all years). This indicates that the peripheral community structure (away from the network core) of the EBA financial network is indeed strongly aligned with geographic and regional divisions in Europe. We have highlighted two different regional groups in Figure 2.B and 2.C to illustrate the association between angular coordinate and regional structure.

Network structure over time

The longitudinal structure of the data set allows us to track changes in the network structure over the whole time span of observations from 2014 to 2018. Note, however, that the samples of banks included by the EBA vary substantially in size and – even when restricted to the smallest sample – are not completely overlapping; see Table 2. Nevertheless, the goodness-of-fit of the hyperbolic model (reported in Figure 1.B) is surprisingly stable over all years. This suggests that the hyperbolic model does indeed capture intrinsic qualities of the network, rather than relying on transitory structural artefacts.

We proceed to analyze the temporal changes in the latent radial coordinate r' and angular coordinate θ' , corresponding to changes in systemic importance and community structure. Note that the small sample of banks included in the 2016 stress test restricts the number of banks that are included in this longitudinal analysis, cf. Table 2. The scatter plots in Figure 3 and the corresponding Pearson's correlations of .678 between 2014 and 2016 ($P < .0001$) and .569 between 2016 and 2018 ($P = .0001$) show a clear positive association between hyperbolic centrality in successive snapshots of the financial networks. In panel A of Figure 3, Nordea bank can be identified as a clear outlier, moving from a very central position in 2014 to a peripheral position in 2016. Interestingly, Nordea was one of just two banks (together with Royal Bank of Scotland) which were removed from the list of G-SIBs in the subsequent update in 2018 due to decreasing systemic importance.²⁹



Figure 3. Changes in radial coordinate r' (low values indicate high centrality) between 2014 and 2016 (A) and 2016 and 2018 (B). Banks considered systemically relevant (G-SIBs) at the end of the time period are marked in red. Nordea bank is circled in the panel A; see text for background.

For the angular coordinate, we account for the circular nature of the variable and compute the *circular correlation*³⁰ of the angular coordinates between successive years. A moderate association between successive years can be observed at circular correlation values of 0.211 between 2014 and 2016 ($P = .1877$) and 0.225 between 2016 and 2018 ($P = 0.1385$).

Discussion

Based on data from the EBA stress tests of 2014, 2016 and the transparency exercise of 2018, we have presented strong evidence that the latent geometry of financial networks can be well-represented by geometry of negative curvature, i.e., by hyperbolic geometry. Calculating stress-minimizing embeddings into the Poincaré disc model of hyperbolic geometry has allowed us to visualize this geometric structure and to connect it to the popularity-vs-similarity model of Papadopoulos et al.⁴ We find that the radial coordinate (*'popularity'*) is strongly associated with systemic importance (as assessed by the Financial Stability Board) and the angular coordinate (*'similarity'*) with geographic and regional subdivisions. A longitudinal analysis shows that – in the observation period from 2014 to 2018 – systemic importance of banks within the European banking network has stayed rather stable and has been predominated by only gradual changes. The peripheral community structure has been more variable, but

has remained strongly determined by geographical divisions in all years considered.

In future research we plan to study the interplay between hyperbolic network geometry and the dynamics of contagion processes. We are confident, that the empirical analysis of latent network geometry in this paper can provide the basis for new analytic models for the diffusion of financial stress in a banking network with hyperbolic structure.

Methods

Data Preparation and Inference of Financial Networks

The financial networks were extracted from three different publicly available data sets stemming from the stress tests (in 2014 and 2016) and the EU-wide transparency exercise (in 2018) of the European Banking Authority (EBA).^{12,13} The data sets contain detailed balance sheet information from all European banks (EU + Norway) included in the stress test/transparency exercise of the EBA in the respective year. From these data sets we extracted the portfolio values of all sovereign bonds held by the banks, split by issuing country (38 countries) and three levels of maturity (short: 0M-3M, medium: 3M-2Y, long: 2Y-10Y+), resulting in $m = 38 \times 3 = 114$ different asset classes.

For each year, this data was stored as the weighted adjacency matrix P ('portfolio matrix') of a bipartite network. The n rows of P correspond to the banks in the sample, the m columns to the different asset classes, and the element P_{ik} to the portfolio value (in EUR) of asset k in the balance sheet of bank i . To perform a one-mode projection of this bipartite network, we followed Cont and Wagalath^{20,31} as well as Cont and Schaanning¹⁹: We computed the liquidity-weighted portfolio overlap (LWPO) of bank i and bank j as

$$L_{ij} = \sum_{k=1}^m \frac{P_{ik}P_{jk}}{d_k}, \quad (1)$$

where d_k is the market depth for asset k .¹⁹ The LWPO measures the impact of a sudden liquidation of the portfolio of bank i on the portfolio value of bank j and vice versa. Hence, it quantifies the risk of fire-sale contagion between the banks in a financial stress scenario. The market depth of asset k was estimated from P as its total volume held by all banks in the sample, i.e., as $d_k = \sum_{i=1}^n P_{ik}$. Writing D for the diagonal matrix of market depths, (1) can be succinctly written as matrix product $L = PD^{-1}P^T$. Finally, we set the link weight w_{ij} between bank b_i and b_j in the one-mode projection N of the banking network equal to the normalized LWPO between banks b_i and b_j , i.e., $w_{ij} := L_{ij} / \max_{i,j} L_{ij}$

Background on hyperbolic geometry

The hyperboloid model

Hyperbolic geometry can be characterized as the geometry of a space of constant *negative* curvature, while the more familiar Euclidean geometry is the geometry of a flat space, i.e. a space of zero curvature. In the *hyperboloid model* of hyperbolic geometry^{32,33}, d -dimensional hyperbolic space \mathbb{H}_d is defined as the hyperboloid

$$\mathbb{H}_d = \left\{ x \in \mathbb{R}^{d+1} : x_0^2 - x_1^2 - \dots - x_d^2 = 1, x_0 > 0 \right\} \quad \text{equipped with distance} \quad d_H(x, y) = \operatorname{arcosh}(x_0y_0 - x_1y_1 - \dots - x_dy_d).$$

In fact, \mathbb{H}_d endowed with the Riemannian metric tensor $ds^2 = dx_0^2 - dx_1^2 - \dots - dx_d^2$ is a Riemannian manifold and $d_H(x, y)$ is the corresponding Riemannian distance.^{32,33} The sectional curvature of this manifold is constant and equal to -1 . Thus, \mathbb{H}_d is indeed a model of geometry of constant negative curvature.

The Poincaré disc model

While the hyperboloid model is convenient for computations, a more preferable (and popular) model for visualizations in dimension $d = 2$ is the *Poincaré disc model*³², which also forms the basis of the popularity-vs-similarity model of Papadopoulos et al.⁴. To obtain the Poincaré disc model, the hyperboloid \mathbb{H}_2 is mapped to the open unit disc ('Poincaré disc') $\mathbb{D} = \{z \in \mathbb{R}^2 : z_1^2 + z_2^2 < 1\}$, parameterized by polar coordinates as $z_1 = r \cos \theta$, $z_2 = r \sin \theta$, using the *stereographic projection* (cf. [32, §4.2])

$$r = \sqrt{\frac{x_0 - 1}{x_0 + 1}}, \quad \theta = \operatorname{atan}'(x_2, x_1), \quad x = (x_0, x_1, x_2) \in \mathbb{H}_2, \quad (2)$$

	2014	2016	2018
number of banks (n)	119	51	128
of which included in the subseq. year	43	41	

Table 2. Sample sizes of EBA data sets

where atan' is the quadrant-preserving arctangent.* In the Poincaré disc model, the hyperbolic distance becomes

$$d_B((r_1, \theta_1), (r_2, \theta_2)) = \text{arcosh} \left(1 + 2 \frac{r_1^2 + r_2^2 + 2r_1 r_2 \cos(\theta_1 - \theta_2)}{(1 - r_1^2)(1 - r_2^2)} \right)$$

and geodesic lines are represented by arcs of (Euclidean) circles intersected with \mathbb{D} .

Hyperbolic Embedding and Centering

Embedding into Hyperbolic Space

Network embedding methods aim to find – for each network node b_i – latent coordinates x^i in a geometric model space G , such that the geodesic distance between x^i and x^j in G matches – as closely as possible – a given dissimilarity measure d_{ij} between nodes b_i and b_j . Stress-minimizing embedding methods aim to minimize the stress functional

$$\text{Stress}(x^1, \dots, x^n) = \sqrt{\frac{1}{n(n-1)} \sum_{i,j} \left(d_{ij}^{\text{network}} - d_G^{\text{geom}}(x^i, x^j) \right)^2}, \quad (3)$$

which measures the root mean square error between given network dissimilarities and the corresponding distances in the model space. For Euclidean geometry, this method is well-known as multidimensional scaling^{21,34}, or – using a weighted stress functional – as Sammon mapping³⁵. For hyperbolic space, i.e., when $d_G^{\text{geom}} = d_H$, several optimization methods for (3) have been proposed^{22,23,36}. We use the `hydra` method implemented in the package `hydra` for the statistical computing environment `R`³⁷.

Hyperbolic Centering

For a point cloud x^1, \dots, x^n in \mathbb{H}_d and non-negative weights w_1, \dots, w_n summing to one, the *hyperbolic mean*³⁰ or *hyperbolic center of weight*³⁸ can be determined as follows: Calculate the weighted Euclidean mean $\bar{x} = \sum w_i x^i$, and its ‘resultant length’ $\rho = \sqrt{(\bar{x}_0)^2 - (\bar{x}_1)^2 - \dots - (\bar{x}_d)^2}$, which is a measure of dispersion for the point cloud. The hyperbolic center c is then determined as $c = \bar{x}/\rho$ and is again an element of \mathbb{H}_d . The point cloud can be centered at c by transforming each points as $(x^i)' = T_{-c} x^i$, where T_c is the hyperbolic translation matrix (‘Lorentz boost’)

$$T_c = \begin{pmatrix} c_0 & \bar{c}^\top \\ \bar{c} & \sqrt{I_d + \bar{c}\bar{c}^\top} \end{pmatrix} \quad \text{with} \quad c = (c_0, \bar{c}) = (c_0, c_1, \dots, c_d).$$

In dimension $d = 2$, the stereographic projection (2) may then be applied to convert the centered coordinates $(x^i)'$ to centered polar coordinates (r'_i, θ'_i) in the Poincaré disc.

Application to Financial Networks

The described methods were applied to the financial networks inferred from the EBA data as follows: We converted the similarity weights w_{ij} (normalized LWPO) to dissimilarities $d_{ij} = 1 - w_{ij}$. We embedded these similarities by minimizing the stress functional (3), using the `R`-package `hydra`. For the resulting network embeddings, we calculated the capital-weighted network center c as the weighted hyperbolic mean with weights w_i proportional to the total capital $\sum_{k=1}^m P_{ik}$ of bank i invested in all assets a_1, \dots, a_m . After centering at the hyperbolic center c , we calculated the coordinates (r'_i, θ'_i) by the stereographic projection (2).

Data Availability Statement

The data analysed during the current study are available from the website of the European Banking Authority at <https://www.eba.europa.eu/risk-analysis-and-data/eu-wide-stress-testing> and <https://eba.europa.eu/risk-analysis-and-data/eu-wide-transparency-exercise/2018>.

References

1. Shavitt, Y. & Tankel, T. On the curvature of the internet and its usage for overlay construction and distance estimation. In *IEEE INFOCOM 2004*, vol. 1 (IEEE, 2004).
2. Muscoloni, A., Thomas, J. M., Ciucci, S., Bianconi, G. & Cannistraci, C. V. Machine learning meets complex networks via coalescent embedding in the hyperbolic space. *Nat. communications* **8**, 1–19 (2017).

*The quadrant-preserving arctangent $\text{atan}'(x_2, x_1)$, well-defined unless $x_1 = x_2 = 0$, returns the unique angle $\theta \in [0, 2\pi)$ which solves $\tan \theta = x_2/x_1$ and points to the same quadrant as (x_1, x_2) . It is commonly implemented in scientific computing environments (e.g. in `MATLAB` or `R`) as `atan2`.

3. Alanis-Lobato, G., Mier, P. & Andrade-Navarro, M. A. Manifold learning and maximum likelihood estimation for hyperbolic network embedding. *Appl. network science* **1**, 1–14 (2016).
4. Papadopoulos, F., Kitsak, M., Serrano, M. Á., Boguná, M. & Krioukov, D. Popularity versus similarity in growing networks. *Nature* **489**, 537 (2012).
5. Papadopoulos, F., Psomas, C. & Krioukov, D. Network mapping by replaying hyperbolic growth. *IEEE/ACM Transactions on Netw. (TON)* **23**, 198–211 (2015).
6. Barabasi, A.-L. Luck or reason. *Nature* **486**, 507–509 (2012).
7. Brockmann, D. & Helbing, D. The hidden geometry of complex, network-driven contagion phenomena. *Science* **342**, 1337–1342 (2013).
8. Cont, R., Moussa, A. & Santos, E. B. Network structure and systemic risk in banking systems. In Jean-Pierre Fouque, J. A. L. (ed.) *Network Structure and Systemic Risk in Banking Systems* (Cambridge University Press, 2010).
9. Battiston, S., Gatti, D. D., Gallegati, M., Greenwald, B. & Stiglitz, J. E. Liaisons dangereuses: Increasing connectivity, risk sharing, and systemic risk. *J. economic dynamics control* **36**, 1121–1141 (2012).
10. Roukny, T., Bersini, H., Pirotte, H., Caldarelli, G. & Battiston, S. Default cascades in complex networks: Topology and systemic risk. *Sci. reports* **3**, 2759 (2013).
11. French, K. *et al.* The Squam Lake report: fixing the financial system. *J. Appl. Corp. Finance* **22**, 8–21 (2010).
12. European Banking Authority. EU-wide stress testing. <https://www.eba.europa.eu/risk-analysis-and-data/eu-wide-stress-testing>.
13. European Banking Authority. EU-wide transparency exercise. <https://eba.europa.eu/risk-analysis-and-data/eu-wide-transparency-exercise/2018>.
14. Caccioli, F., Farmer, J. D., Foti, N. & Rockmore, D. Overlapping portfolios, contagion, and financial stability. *J. Econ. Dyn. Control* **51**, 50–63, DOI: [10.1016/j.jedc.2014.09.041](https://doi.org/10.1016/j.jedc.2014.09.041) (2015).
15. Eisenberg, L. & Noe, T. H. Systemic risk in financial systems. *Manag. Sci.* **47**, 236–249 (2001).
16. Brown, M., Trautmann, S. T. & Vlahu, R. Understanding bank-run contagion. *Manag. Sci.* **63**, 2272–2282 (2017).
17. Shleifer, A. & Vishny, R. W. Liquidation Values and Debt Capacity: A Market Equilibrium Approach. *The J. Finance* **47**, 1343–1366, DOI: [10.1111/j.1540-6261.1992.tb04661.x](https://doi.org/10.1111/j.1540-6261.1992.tb04661.x) (1992).
18. Glasserman, P. & Young, H. P. How likely is contagion in financial networks? *J. Bank. Finance* **50**, 383–399, DOI: [10.1016/j.jbankfin.2014.02.006](https://doi.org/10.1016/j.jbankfin.2014.02.006) (2015).
19. Cont, R. & Schaanning, E. Fire sales, indirect contagion and systemic stress testing (2017). Norges Bank Working Paper 02/2017.
20. Cont, R. & Wagalath, L. Fire sales forensics: measuring endogenous risk. *Math. Finance* **26**, 835–866 (2016).
21. Kruskal, J. B. & Wish, M. *Multidimensional scaling*, vol. 11 (Sage, 1978).
22. Chowdhary, K. & Kolda, T. G. An improved hyperbolic embedding algorithm. *J. Complex Networks* **6**, 321–341 (2017).
23. Keller-Ressel, M. & Nargang, S. Hydra: a method for strain-minimizing hyperbolic embedding of network-and distance-based data. *J. Complex Networks* **8**, cnaa002 (2020).
24. Krioukov, D., Papadopoulos, F., Kitsak, M., Vahdat, A. & Boguná, M. Hyperbolic geometry of complex networks. *Phys. Rev. E* **82**, 036106 (2010).
25. Boss, M., Elsinger, H., Summer, M. & Thurner, S. Network topology of the interbank market. *Quant. finance* **4**, 677–684 (2004).
26. Langfield, S., Liu, Z. & Ota, T. Mapping the UK interbank system. *J. Bank. & Finance* **45**, 288–303 (2014).
27. Financial Stability Board. 2014 update of list of global systemically important banks (G-SIBs). <https://www.fsb.org/2014/11/2014-update-of-list-of-global-systemically-important-banks/>.
28. Financial Stability Board. 2016 list of global systemically important banks (G-SIBs). <https://www.fsb.org/2016/11/2016-list-of-global-systemically-important-banks-g-sibs/>.
29. Financial Stability Board. 2018 list of global systemically important banks (G-SIBs). <https://www.fsb.org/2018/11/2018-list-of-global-systemically-important-banks-g-sibs/>.
30. Mardia, K. V. & Jupp, P. E. *Directional statistics* (John Wiley & Sons, 2009).

31. Cont, R. & Wagalath, L. Running for the exit: distressed selling and endogenous correlation in financial markets. *Math. Finance: An Int. J. Math. Stat. Financial Econ.* **23**, 718–741 (2013).
32. Ratcliffe, J. G. *Foundations of hyperbolic manifolds*, vol. 3 (Springer, 1994).
33. Cannon, W. J., Floyd, W. J., Kenyon, R. & Parry, W. R. Hyperbolic geometry. In Silvio Levy (ed.) *Flavors of Geometry*, 59–115 (MSRI Publications, 1997), 31 edn.
34. Borg, I. & Groenen, P. Modern multidimensional scaling: Theory and applications. *J. Educ. Meas.* **40**, 277–280 (2003).
35. Sammon, J. W. A nonlinear mapping for data structure analysis. *IEEE Transactions on computers* **100**, 401–409 (1969).
36. Zhao, X., Sala, A., Zheng, H. & Zhao, B. Y. Fast and scalable analysis of massive social graphs. *arXiv preprint arXiv:1107.5114* (2011).
37. R Core Team. *R: A Language and Environment for Statistical Computing*. R Foundation for Statistical Computing, Vienna, Austria (2019).
38. Galperin, G. A concept of the mass center of a system of material points in the constant curvature spaces. *Commun. Math. Phys.* **154**, 63–84 (1993).

Author contributions statement

M.K.R. conceived the study, S.N. prepared the data, M.K.R. and S.N. analysed the results. All authors reviewed the manuscript.

Additional information

The author(s) declare no competing interests.

AT01	Erste Group Bank AG	GR01	Eurobank Ergasias
AT08	BAWAG Group AG	GR02	National Bank of Greece
AT09	Raiffeisen Bank International AG	GR03	Alpha Bank
AT10	Raiffeisenbankengruppe Verbund eGen	GR04	Piraeus Bank
AT11	Sberbank Europe AG	HU01	OTP Bank Ltd
AT12	Volksbanken Verbund	IE04	AIB Group plc
BE01	Belfius Banque SA	IE05	Bank of Ireland Group plc
BE02	Dexia NV	IE06	Citibank Holdings Ireland Limited
BE04	AXA Bank Europe SA	IE07	DEPFA BANK Plc
BE06	KBC Group NV	IS01	Arion banki hf
BE07	The Bank of New York Mellon SA/NV	IS02	Íslandsbanki hf.
BE08	Investar	IS03	Landsbankinn
BG01	First Investment Bank	IT01	Intesa Sanpaolo S.p.A.
CY01	Hellenic Bank Public Company Ltd	IT02	UniCredit S.p.A. *
CY04	Bank of Cyprus Holdings Public Limited Company	IT03	Banca Monte dei Paschi di Siena S.p.A.
CY05	RCB Bank Ltd	IT04	Unione Di Banche Italiane Società Cooperativa Per Azioni
DE01	NRW.Bank	IT05	Banca Carige S.P.A. - Cassa di Risparmio di Genova e Imperia
DE02	Deutsche Bank AG *	IT07	Banca Popolare Dell'Emilia Romagna - Società Cooperativa
DE03	Commerzbank AG	IT09	Banca Popolare di Sondrio
DE04	Landesbank Baden-Württemberg	IT13	Mediobanca - Banca di Credito Finanziario S.p.A.
DE05	Bayerische Landesbank	IT16	Banco BPM Gruppo Bancario
DE06	Norddeutsche Landesbank-Girozentrale	IT17	Credito Emiliano Holding SpA
DE07	Landesbank Hessen-Thüringen Girozentrale	IT18	Iccrea Banca Spa Istituto Centrale del Credito Cooperativo
DE08	DekaBank Deutsche Girozentrale	LU01	Banque et Caisse d'Épargne de l'Etat
DE09	Aareal Bank AG	LU02	Precision Capital S.A.
DE10	Deutsche Apotheker- und Ärztebank eG	LU03	J.P. Morgan Bank Luxembourg S.A.
DE11	HASPA Finanzholding	LU04	RBC Investor Services Bank S.A.
DE14	Landescreditbank Baden-Württemberg-Förderbank	LU05	State Street Bank Luxembourg S.A.
DE15	Landwirtschaftliche Rentenbank	MT01	Bank of Valletta plc
DE16	Münchener Hypothekenbank eG	MT02	Commbank Europe Ltd
DE20	DZ Bank AG Deutsche Zentral-Genossenschaftsbank	MT03	MDB Group Limited
DE25	Deutsche Pfandbriefbank AG	NL01	Bank Nederlandse Gemeenten N.V.
DE26	Erwerbsgesellschaft der S-Finanzgruppe mbH & Co. KG	NL02	Coöperatieve Centrale Raiffeisen-Boerenleenbank B.A.
DE27	SHS Beteiligungs Management GmbH	NL03	Nederlandse Waterschapsbank N.V.
DE28	State Street Europe Holdings Germany S.à.r.l. & Co. KG	NL07	ABN AMRO Group N.V.
DE29	Volkswagen Bank GmbH	NL08	ING Groep N.V. *
DK01	Danske Bank	NL09	Volksholding B.V.
DK02	Jyske Bank	NO01	DNB Bank Group
DK03	Sydbank	NO02	SPAREBANK 1 SMN
DK05	Nykredit Realkredit	NO03	SR-bank
EE01	AS LHV Group	PL01	PKO BANK POLSKI
ES01	Banco Santander *	PL07	Bank Polska Kasa Opieki SA
ES02	Banco Bilbao Vizcaya Argentaria	PT01	Caixa Geral de Depósitos
ES03	Banco de Sabadell	PT02	Banco Comercial Português
ES04	Banco Financiero y de Ahorros	PT04	Caixa Central de Crédito Agrícola Mútuo, CRL
ES07	Caja de Ahorros y M.P. de Zaragoza	PT05	Caixa Económica Montepio Geral, Caixa Económica Bancária SA
ES08	Kutxabank	PT06	Novo Banco, SA
ES09	Liberbank	RO01	Banca Transilvania
ES11	MPCA Ronda	SE01	Nordea Bank AB (publ) †
ES12	Caja de Ahorros y Pensiones de Barcelona	SE02	Skandinaviska Enskilda Banken AB (publ) (SEB)
ES15	Bankinter	SE03	Svenska Handelsbanken AB (publ)
ES18	Abanca Holding Financiero, S.A.	SE04	Swedbank AB (publ)
ES19	Banco de Crédito Social Cooperativo, S.A.	SE05	Kommuninvest - group
FI01	OP-Pohjola Group	SE06	Länsförsäkringar Bank AB - group
FI02	Kuntarahoitus Oyj	SE07	SBAB Bank AB - group
FR01	La Banque Postale	SI02	Nova Ljubljanska banka d. d.
FR02	BNP Paribas *	SI04	Abanka d.d.
FR03	Société Générale *	SI05	Biser Topco S.à.r.l.
FR06	C.R.H. - Caisse de Refinancement de l'Habitat	UK01	Royal Bank of Scotland Group plc †
FR08	RCI Banque	UK02	HSBC Holdings plc *
FR09	Société de Financement Local	UK03	Barclays plc *
FR12	Groupe Crédit Mutuel	UK04	Lloyds Banking Group plc
FR13	Banque Centrale de Compensation (LCH Clearmet)	UK05	Nationwide Building Society
FR14	Bpifrance (Banque Publique d'Investissement)	UK06	Standard Chartered Plc *
FR15	Groupe BPCE *		
FR16	Groupe Crédit Agricole *		

Table 3. IDs and full names of banks in the 2018 EBA Network. Banks marked by asterisk (*) were G-SIBs in all years (2014, 2016, 2018); banks marked by dagger (†) were G-SIBs in 2014 and 2016, but not in 2018.